

Analysis of 3-D Printed Structural Components for Cube Satellites

C. Herzfeld

SPAWAR SYSTEMS CENTER (SSC) ATLANTIC, Charleston, SC, USA

Claudio.Herzfeld@navy.mil

Abstract: Additive manufacturing uses 3-D printing to build physical parts from CAD-based designs. The technology includes fused deposition modeling (FDM) and selective laser sintering (SLS) methods. 3-D printing is of particular interest for smaller, one-of-a-kind, customizable products. A cube satellite (CubeSat) containing fiber reinforced SLS parts has been successfully launched (Ref 1).

Lower cost FDM can be less attractive for manufacturing CubeSat components, since the FDM materials cannot be fiber reinforced, and the mechanical properties are not close to aluminum. One industry solution has been to coat the 3-D printed parts. The mechanical properties can be greatly improved by electroplating a metal coating to form a sandwich composite structure. Additional benefits include EMI shielding, increased temperature capability, elimination of outgassing and reduced flammability. To properly design and analyze the component structure, the output geometry of electroplating analysis must be imported into a structural mechanics module. The research investigates performing the analysis within the framework of the COMSOL Multiphysics software.

Keywords: electroplating models, structural shells, 3-D printing, CubeSat

1. Introduction

Government and Industry are focused on reducing the development time and costs for bringing new products to realization. One rapidly expanding technology sector uses 3-D printing (additive manufacturing) for turning CAD-based designs and models into a physical object. Initial 3-D printed products (e.g. stereolithography SLA) were typically brittle “models” and offered minimal mechanical performance. Today the technology has matured and current products include fused deposition modeling (FDM) and selective laser sintering (SLS) methods. FDM deposits and fuses beads of molten thermoplastic to build prototype and limited production commercial parts, while SLS uses a moving laser beam to sinter plastic or

metal powder layers heated close to the fusion point to build the part. Recent interest has focused on using 3-D printing in space technology e.g. for manufacturing cube satellite structural components (Ref 2).

CubeSats were developed as a means to standardize satellite buses, structures, and subsystems. A CubeSat is a 10 cm cube with a mass of up to 1 kg. This size falls well within the capability of commercial 3-D printers. The unique cube shape allows satellite systems to be built up by attaching 2-6 cubes together or simply using a single cube. The CubeSat structural frame is assembled from aluminum components (Ref 3).

While FDM has greater consumer and market appeal due to the lower cost of machines and materials, lower process temperatures and manufacturing simplicity, SLS has been more successful in aerospace applications where fiber reinforcements are critical to improve strength to weight ratios.

For his master’s thesis, D. Fluitt performed a 3-D printing trade study and tensile tested candidate materials for CubeSat applications (Ref 4). Materials included Windform XT, a carbon fiber filled nylon and ABS plastic. Windorm XT processed by SLS was the most expensive material, and ABS plastic processed by FDM one of the cheapest. Not surprisingly, Windform XT has superior performance compared to ABS. A CubeSat containing Windform XT parts has been successfully launched (Ref 1).

Mr. Fluitt was critical of the anisotropic nature of ABS and generalized his conclusions to all FDM parts. This is illustrated in a paper by A. Bagsik et al. for ULTEM 9085 (Ref 5). The tensile data showed a Max/Min ratio of at least 2:1 for tensile strength and elongation for horizontal X-axis versus vertical Z-axis orientation. Mechanical weakness in the z-plane has to be taken into consideration when designing FDM parts.

This major deficiency of FDM may be overcome by adding a structural metal coating (e.g. via electroplating). The process has proved valuable for extending the mechanical properties and life of the more brittle SLA materials, e.g. a

SLA part arm that failed in less than 30 cycles completed 400,000 cycles in a commercial postal addressing machine after electroplating with nickel (Ref 6 and 7). Nylon SLS parts are also plated, and a 10x strength increase and increased stiffness comparable to aluminum can be obtained. (Ref 8 and 9). Typically a copper coating is applied for electrical and thermal conductivity due to its faster and more even plating distribution. Then a nickel coating is added for hardness and mechanical strength. Turnaround for 3-D printing and electroplating parts can be less than 24 hours for each process step.

Metal coated SLA materials have been used in spaceflight applications (Ref 10). "The assembled system was rigorously tested in the lab, and followed a standard process for the verification of flight parts, including vibration testing to proto-flight levels (in stowed condition), thermal cycling, EMI, Acoustic, Sharp Edge Inspection and Off-gas Testing (NAS-STD-6001 Test 1). The project also took advantage of these materials to create EMI shields. It was realized after preliminary EMI evaluation was performed that certain components of the equipment needed shields that contained relatively complex geometries. Ni clad 3-D printed materials offered an excellent, low cost and low weight solution to this problem".

While metal coated 3-D printed materials have made great strides in gaining customer acceptance, one critical technology gap still exists today, the inability to accurately model and predict the structural benefits of the metal coatings on the mechanical and thermal properties of complex 3-D printed plastic parts. 3-D printed materials remain porous with innumerable fusion welds, so the metal coatings make all the difference in material performance, but structural metal coatings are still applied today more by "rule of thumb" or guesswork versus rigorous structural design.

The benefits of analyzing the structural properties of metal-coated 3-D printed parts include: a) being able to quantify the performance improvements obtainable with the metal coatings, b) making an informed choice between uncoated versus plated parts, c) obtaining a better optimization of the final design properties, d) reducing development time and cost with less need for testing, and e)

extending the use of 3-D printed parts to new applications.

2. Use of COMSOL Multiphysics

Multiphysics modeling and simulation were performed using COMSOL Multiphysics 4.4 and the CAD Import, Electrodeposition and Structural Mechanics modules. Due to the nested model structure, selections were primarily performed in wireframe mode using the selection box feature.

a) CAD Import Module

- The CAD Import module was used to import CAD geometry files under the geometry node. A fixed electroplating tank geometry modeled the tank and anode surfaces and various part geometries modeled the cathode surfaces. The representative cathode geometry was an array of 5 x 3 parts, e.g. 15 tensile bars. The imported CAD files were parasolids file format. The immersed parts were physically free-floating in the tank.
- Under the geometry node, the difference operator was used to subtract the part geometry from the tank geometry and define the electroplating cell domain. The original tank domain was deleted.
- The imported part domains were retained and used in the structural mechanics analysis. Subsequently, the tensile bars were split into 3 domains each in CAD to make the reduced tensile section a separate domain for analysis.
- The two part CAD import procedure was used to import a Cubsat support bracket geometry file. Rotation and translation operators were used to immerse the plate in the tank. Defeaturing operators were used to remove tapered countersinks and threaded bolt faces and reduce edge complexity.

b) Electrodeposition Module

- The Electrodeposition, Deformed Geometry, Secondary (edsec) physics node was used to simulate electroplating copper and/or nickel on the cathode surfaces of the electroplating cell, e.g. the 15 tensile bars. The electrodeposition physics node was set up following the COMSOL example steps for decorative nickel plating.

- The plating parameters were selected from experience with a legacy code. Both codes use the Butler-Volmer equation to compute activation polarization, but define different initial conditions. COMSOL specifies the average current density, while the legacy code specifies the applied cell potential.
- The outputs for both codes are plating thickness values defined at the cathode surface mesh nodes. The COMSOL mesh density was approx. twice that of the legacy code.
- The thickness outputs from COMSOL and the legacy code were compared for the 15 tensile bars model. The nodal results were exported into Excel spreadsheets, and the average plating thickness was computed for each tensile bar. The average plating thickness was also solved for in COMSOL by box selecting tensile bar surfaces and calculating the average.

c) Transition between Physics Modules

- The Electrodeposition study and the Structural Mechanics study can be separate studies performed sequentially on the same model.
- Only one meshing operation is performed across all domains. The domains only share common mesh surfaces at the cathode part surfaces.
- The plating thickness results (edsec.sbtot) were used to define variable thickness shells in the Structural Mechanics module.
- The electroplating simulation is performed on the electroplating cell domain, while the structural mechanics analysis of the plated shells is performed on the imported part domains, e.g. the 15 tensile bars. The domains share the cathode/part mesh surfaces, but do not overlap.
- The electrodeposition and the structural mechanics physics analysis are performed in sequence. The modules were not coupled interactively.
- One issue was importing the results of the time-dependent analysis with 3, 6, 9 and 12 hour time steps into a stationary analysis. This was achieved by selecting a single time step in the second Study node.

d) Structural Mechanics Module

- The Solid Mechanics node and two Shell nodes were used to perform linear elastic analysis on the imported and plated parts, e.g. the tensile bars.
- The model consisted of a solid thermoplastic body and two electroplated metal shells. The thermoplastic body properties were defined using a linear material node.
- Unfortunately a material node cannot be associated with the Shell physics nodes, so only linear elastic material properties could be defined within the Shell physics nodes.
- The nodal mesh output of the electrodeposition module was used to define a variable shell thickness. For model simplicity the copper thickness was fixed constant, and only the nickel thickness was variable.
- For tensile load analysis, all 15 tensile bars were equally loaded and solved simultaneously. Surface stress results were localized to the 15 reduced sections using a 3 domain tensile bar model.
- For Eigenfrequency analysis, only a few tensile bars solved simultaneously.
- Linear buckling analysis was performed on a single tensile bar with a small lateral load as illustrated for the COMSOL linear buckling example.

3) Modeling and Simulation Results

Modeling and simulation results are summarized in the tables and figures.

a) CAD Import Module

The model was imported as two files. The final result is illustrated in Fig. 1. The second file import immersed the part geometry (tensile bar array) in the fixed electroplating tank geometry. Any CAD non-symmetric part geometry/array may be used. Subtracting the part geometry in COMSOL created a new plating cell domain by difference, while retaining the original part domains. The domains share common surfaces used in defining the cathodes for electrodeposition and the plated shells in structural mechanics.

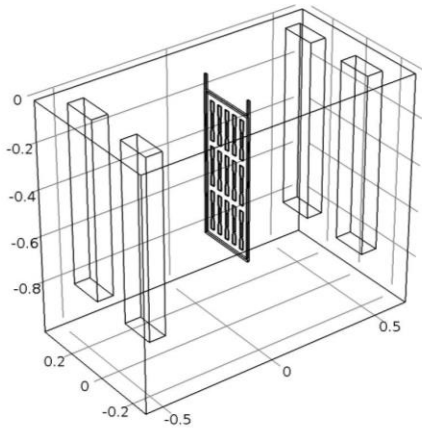


Fig. 1 Electroplating Tank Geometry

The model was meshed using a physics controlled mesh as illustrated in Fig. 2. The mesh had twice as many nodes/tensile bar as a comparison model using the legacy code.

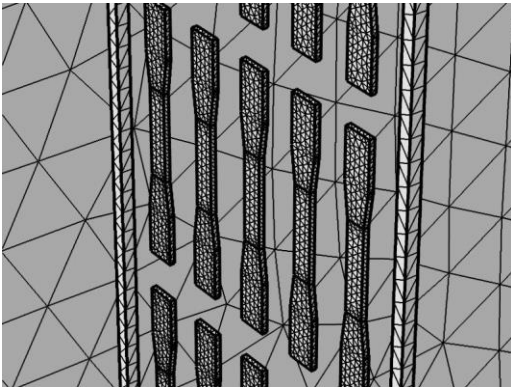


Fig. 2 Physics Controlled Mesh

b) Electrodeposition Module

The results of 3 hours copper electroplating are illustrated in Fig. 3. Note the non-uniform plating on the sides and bottom of the array. This is a worst-case example and not characteristic of what can be achieved with commercial electroplating. The average nodal thickness results for each of the 15 tensile bars were compared to the legacy code (3 hours and 12 hours plating). There is excellent agreement between the two simulation codes (Maximum +/- 0.3% difference in average thickness results).

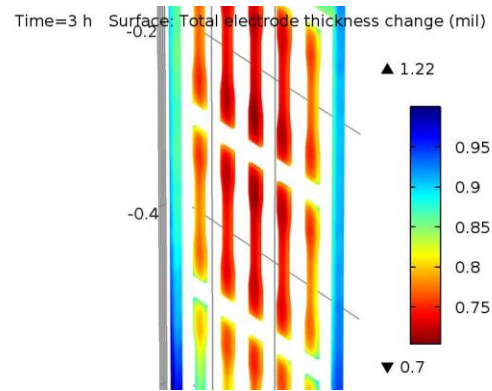


Fig. 3 Copper Electroplating (mils)

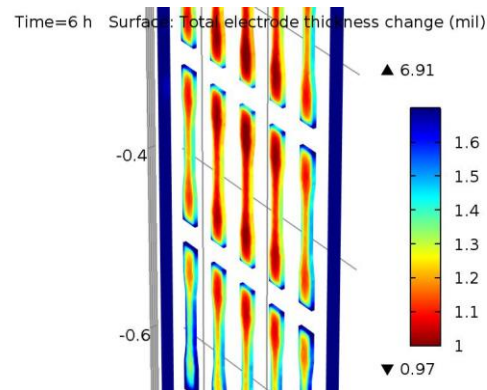


Fig. 4 Nickel Electroplating (mils)

The results of 6 hours nickel electroplating are illustrated in Fig. 4. Note the plating uniformity is worse than copper for similar plating thickness ($25.4 \mu\text{m} = 1 \text{ mil}$). The average nodal thickness results for each of the 15 tensile bars were compared to the legacy code (12 hours plating). The difference between the two simulation codes shows a 4% shift in average thickness values. The cause of the shift was not identified. COMSOL models the H_2 reaction as well as the metallization reaction at the cathode, but deleting the H_2 reaction node caused only negligible improvement, so this was ruled out as the cause of the shift. The increased time step was also ruled out, since the current density distribution (proportional to the plating rate) is invariant with time.

c) Structural Mechanics Module

A linear elastic structural mechanics analysis was performed on the tensile bar array as illustrated in Figs. 5-7. An 890 N (200lbf) load

was applied to each Ultem 9085 core electroplated with 3 mils of copper and 1 mil of nickel. The nickel shell thickness was defined by the edsec.sbtot output of the electroplating study. Fig 5 illustrates the Von Mises stress in the low modulus 3-D printed Ultem 9085 tensile bar core. The high stress at the top of the bar is where the load was applied versus applying it more correctly to the grip faces. The average Von Mises stress results were compared to the stresses in the nickel and copper shells.

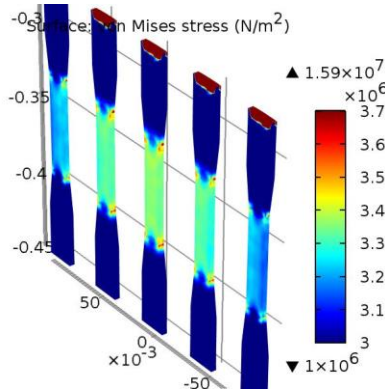


Fig. 5 Von Mises Stress (Solid Core) 890N

Fig. 6 illustrates the stress results in the fixed 3 mil copper shell. Fig. 7 illustrates the stress results in the variable thickness nickel shell. Note the Von Mises stresses in the copper and nickel shells are approx. 50x and 100x larger than in the low modulus Ultem core. In the linear elastic region the metal shells carry the load and not the core. The results were checked to confirm the stress in the shells was below the yield stress of the metals, and the principal strain was low (less than 0.2%).

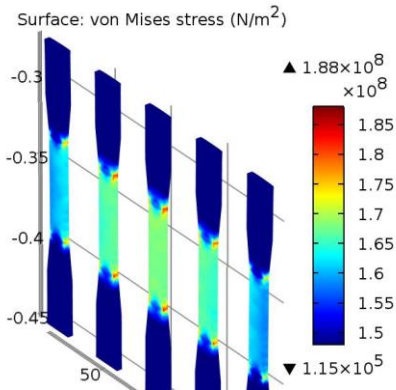


Fig. 6 Von Mises Stress (3 mil Cu Shell) 890N

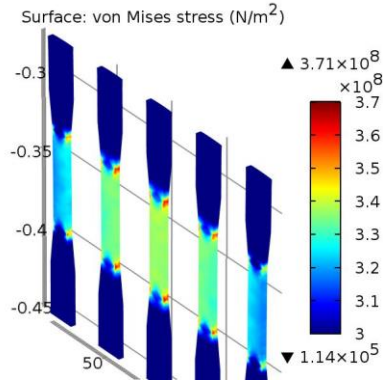


Fig. 7 Von Mises Stress (1 mil Ni Shell) 890N

Fig. 8 illustrates the Von Mises stress results for Ultem 9085 tensile bars without metal plating. The modeling results are consistent for all tensile bars

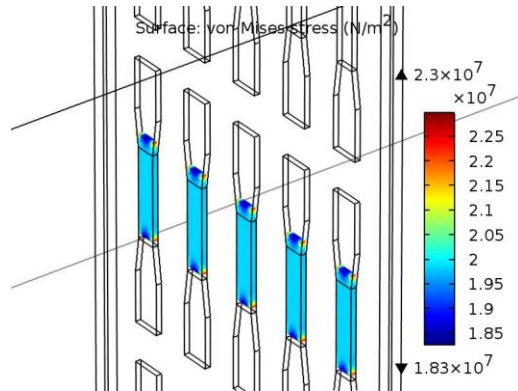


Fig. 8 Von Mises Stress Ultem 9086 No Shells

Comparing the Ultem 9085 tensile “core” results with the Ultem 9085 tensile bar results shows a significant difference:

- The Von Mises stress in the Ultem material under 890 N load is 6x higher without 4 mils of combination plating
- The principal strain (elongation) in the Ultem material under 890 N load is 6x higher without 4 mils of combination plating.
- For metal plated tensile bars the applied load is carried by the metal shells.
- For metal plated tensile bars, within the linear elastic range, the weakness of FDM materials in the z-plane should not be a significant risk factor, since the stress in the core material is so low.

4) Discussion

a) CAD Import Module and Geometry

The parasolids CAD multiple file imports were successful in assembling the model geometry. While the tensile bar geometry was already aligned to the tank geometry, other import geometries were not and had to be rotated and translated to be fully immersed in the tank.

b) Electrodeposition Module

The mirror symmetry of the tank configuration was not used in reducing model complexity for electrodeposition analysis, because other 3-D component parts are expected to be non-symmetric. Furthermore, it is simpler to set up the structural analysis on whole parts.

The major issue with the electroplating analysis is the non-uniformity of the achieved plating. The apparent cause is the mismatch between anode and cathode surface configurations creating a non-linear electrostatic field. The anodes extend beyond the depth of the cathode rack causing increased current density and plating thickness on the bottom row of tensile specimens. Similarly, the anodes are spaced further apart than the width of the cathode rack causing increased plating on the outside tensile bars. The plating uniformity can be greatly improved by proper loading and use of field control elements.

The close agreement between the COMSOL edsec code and the legacy code for copper plating despite the model differences in solving the Butler-Volmer equation is highly satisfactory. The larger differences for nickel plating, in particular the shift in sample average plating thickness requires further investigation. In any case, the plating parameters need to be carefully chosen, so the simulation results can be validated against empirical plating thickness measurements.

c) Structural Mechanics Module

The structural mechanics analysis uses a linear elastic materials model. The structural mechanics results are only valid below the yield stress of the respective materials used. The linear elastic stress in each composite layer is limited by the yield stress for each respective material, but the valid strain range overall for the composite material is limited by the lowest

yielding material, e.g. the highly thermally and electrically conductive copper layer, because of the strain constraint at the material interfaces:

$\epsilon_{\text{Ultem}} = \epsilon_{\text{Cu}} = \epsilon_{\text{Ni}}$. The strain at the interfaces should be the same in the core and shell materials for the plated layers to remain bonded. The limiting model factor appears to be yielding and distortion of the copper shell.

One encouraging result was the stress in the core is approx. 50x lower than the stress in the plated copper shell and 100x lower than the stress in the nickel shell. For the linear elastic model the load is carried by the shells, not the core. This is particularly significant for FDM materials, where the low stress in the core means reduced mechanical properties of FDM in the z-plane should not be an issue.

In tension the metal shells are expected to show non-linear tensile behavior above their yield point. For compression loads, the shells are expected to debond and fail by buckling (when the yield is exceeded). For example, this is typical for metal plated SLA in flexure bending. The results for the COMSOL linear buckling analysis were 3000N = 700lbf, which was considered grossly inaccurate, since it exceeded the yield point of the shells. Non-linear buckling analysis is required.

5) Conclusions:

To summarize::

a) At low strains within the metal elastic range, the load is carried by the metal shells, and there is no significant load on the weaker core. This should in particular benefit FDM materials.

b) At higher tensile strains, the metal coatings exceed the yield stress and deform plastically. The load in the shells reaches a near constant value. Any additional load is carried by the core, which may still increase linearly with increasing load.

c) It should be noted that while the metal coating(s) load non-linearly for plastic deformation, they should still unload fairly linearly (parallel to the elastic range with modulus E). This means e.g. a copper coated core loaded to 1% tensile strain will only unload roughly 0.2% before the coating is forced into compression. The core is still at 0.8% tension. The compressive load in the shell(s) now has to balance the residual tensile load in the core (for net zero load). The metal shell(s) have to be

thick enough to carry the compressive load elastically, or the shells may buckle and fail. The permanent specimen deformation may be roughly estimated at about 0.6% elongation.

Unfortunately, extending the validity of this model beyond 0.2% strain to non-linear materials remains a significant challenge. The major issue is material nodes cannot be associated with the 2-D Shell model nodes. COMSOL offers a separate non-linear structural materials module, but all material nodes have to be associated with 3-D plating layer geometry domains. To create this geometry within COMSOL requires growing the plating surfaces in 3-D using the tertiary Electrodeposition module. COMSOL should be capable of creating this deformed geometry.

6) References

- 1: <http://3dprintingindustry.com/2014/05/09/3d-printing-cube-sat-launch-satellite/>
- 2: Y. Kwon et al. "Direct Manufacturing of CubeSat Using 3-D Digital Printer and Determination of its Mechanical Properties", NPS-MAE-10-006, 12/2010
- 3: R. Kaufman, "3D-Printing a Low-Cost Satellite", <http://www.livescience.com/25044-3d-printing-a-low-cost-satellite.html> 11/26/2012
- 4: D. Fluitt, "Feasibility Study into the Use of 3D Printed Materials in Cubesat Flight Missions", California Polytech M.S. Aerospace Eng. Thesis, 05/2012
- 5: A. Bagsik et al. "Mechanical Properties of Fused Deposition Modeling Parts Manufactured with ULTEM 9085" presented at ANTEC 2011, Boston
- 6: Sean Wise, "Conversation on 5/25/13", sean@repliforminc.com
- 7: S. Wise & R. Connelly, "Prototyping Thin-Walled Metal Parts via Electroforming Over SL Models, RP&M 2004
- 8: Make Larken, "Phone conversation on 5/29/2013", make@nwrapidmfg.com
- 9: NorthWest Rapid Mfg. "SLS FAQs, etc. and Product Information Nylon 12"

<http://www.nwrapidmfg.com/sls-technical-questions/index.html>

- 10: G. Funk, "Metal Coated Rapid Prototype Materials for Spaceflight Applications: Low-Cost, Intricate SLA Parts with 'A' Rated Flammability and Toxic Offgassing", funkg@zin-tech.com
- 11: Sean Wise, "Conversation on 3/5/14", sean@repliforminc.com

7) Future Work

The major challenge remains extending the analysis to non-linear materials. The model tree node structure will require significant changes. In particular, the model geometry has to be modified and new domains created prior to structural mechanics analysis. The new approach should work for both linear and non-linear material nodes. Finally, the model needs to be validated by experimental tensile testing.

8) Acknowledgements

The author wishes to acknowledge the support of SPAWAR (SSC Atlantic) via the NISE program. The NISE technical advisor was Thomas Glaab. The author also thanks contributors Aaron Chang, Tiffany Huang, Isaiah Valentine and Michael Martin.

The author further thanks Sean Wise of Repliform Inc for his encouragement and assistance. Validation samples were prepared by Repliform for future testing.